

# CMANTEC NEURAL NETWORK ALGORITHM BASED CLASSIFICATION OF MAMMOGRAMS USING SLBP

Mr. J. Jeya Caleb<sup>1\*</sup> Dr. M. Kannan<sup>2</sup>

<sup>1</sup>Associate Professor, Dept. of ECE, Saveetha Engineering College, Chennai – 60210

<sup>2</sup>Associate Professor, Dept. of ECE, MIT Campus, Anna University, Chennai – 600044

\*jeycaleb@gmail.com

**Abstract:** A new method for the prediction of breast cancer is presented in this research work which uses Constructive Neural Networks (CNN). As far as the traditional artificial neural networks are concerned, the main problem is in identifying suitable and compact neural network architecture. All previous methods used more layers in the hidden section and also used inter nodes which increased the memory and computational time. The fundamental method i.e. trial and error method still plays a vital role which confronts with two main problems of over-fitting or under-fitting. CNN generates the topology in the training phase by introducing neurons. Here, mammogram images are used from which the texture features are extracted using SLBP (Support Local Binary Pattern). These texture features are then analyzed with predefined learning obtained from neural networks. The best possible combinations of features which can become cancer affected are most likely to be identified as cancer affected cell. These parameters are then used to train the network with the help of CMantec (Competitive Majority Network Trained by Error Correction) algorithm and are thereby used to identify the breast cancer at an improved speed. The effective use of CMantec algorithm brings out efficiently the training process and improves generalization capability for the efficient extraction of texture features of mammogram images.

**Key words:** Constructive Neural Networks, CMantec Algorithm, Mammogram, Texture features, SLBP

## INTRODUCTION

Breast cancer has become one of the most commonly occurring forms of cancer, particularly in women. It accounts for about 25% to 33% of all type of cancers. Identifying the breast cancer in advance stage would help out in appropriate diagnosis, which in turn leads to overcoming the effect of the disease. Proper neural network identification is the greatest challenge faced by the choice of a variety of artificial neural networks. Error based choice results in over fitting or under fitting. Thus, the constructive neural network uses the CMantec algorithm which introduces neurons in the training phase to obtain a compact topology.

The texture features are extracted from the mammogram images [[http : // marathon. csee. usf. edu / Mammography / Database. html](http://marathon.csee.usf.edu/Mammography/Database.html)] and these features are used to train the network so that the network classifies the normal and abnormal mammogram images. In general, the textures features extracted include energy, homogeneity, contrast, correlation, standard deviation, RMS value, cluster prominence, cluster shade etc. The constructive neural network is used to obtain minimally sized architectures (based on the exact requirement) and better generalization capabilities. Thermal perceptron learning rule is used in Cmantec which helps out in constructing architectures in a compact form. To predict estrogen receptor status [Daniel Urda et.al., 2010] CMANTEC was applied.

In this paper, the constructive neural network is explored for better results in the prediction of breast cancer. Section I presents review related to this work. Section II explains the organization of CMantec algorithm, SLBP procedures, and Binarization work outs. The obtained results are exhibited in Section III.

## I. REVIEW OF RELATED WORK

In Cancer, the abnormal cells break up without control and attacks rest of the tissues. The tumor that starts in the breast cells is Breast Cancer. Non cancerous breast lumps are called benign breast lumps. A malignant breast lump, on the other hand, is a cancer cell that can grow into surrounding tissues. Numerous methods can be used for the classification of normal and abnormal mammogram images.

The CAD system helps in early diagnosis of a tumor in the breast. The breast nodules CAD system offer higher classification performance [Chih-Min Lin et.al., 2014].

A fuzzy cerebellar model [Chih-Min Lin and Hsin-Yi Li, 2013] neural network (FCMNN) possess better generalization than conventional fuzzy neural networks. If each layer of FCMNN contains only one different neuron then the FCMNN converges to fuzzy neural networks. Though natural drawbacks of ultrasonic images overcome by the textural feature method, drawback in this method was an accurately fitted architecture because of the trial and error method used in constructing the network.

To optimize artificial neural networks in quantum-based algorithm the main aim was to reduce the connections and also to improve the classification performance [Tzyy-Chyang Lu, 2013]. It had used quantum bits for representation. The connectivity bits do not represent the actual link instead it had indicated the probability of the existence of the connections. Though the quantum-based algorithm could automatically generate the appropriate structure and weights of an ANN, an appropriate stopping criterion related to the quantum bits were missing. This method was found as a complex one.

Probabilistic Spiking Neural Networks (PSNN) was presented as a bench marked method used for speed in convergence and its accuracy. It was able to learn complex datasets using minimal neurons which in turn would help in less hardware when implementation requires, but PSNN was 1.3% less in accuracy than KNN [Hung-Yi Hsieh and Kea-Tiong Tang, 2013] (K-nearest neighbor), which had been accepted in this work even though the memory requirement was 40% less than KNN.

Back-propagation and radial basis function brought together to frame into a novel hybrid algorithm [Vikraman Baskaran et.al., 2011] for prediction. An accuracy of nearly 80% and sensitivity of 88% were observed for the updated algorithm and it was admitted by the author that there was still extent to improve the prediction efficiency which could be attained by efficient learning techniques.

Early detection of breast cancer [Mohammad Sameti et.al., 2009] was proposed in this work.

The feature extraction technique was able to detect signs of cancer development only in 72% of the cases studied. The investigation processes between next to next screenings need to be assigned denser.

Bilateral masking procedures [Paola Casti et.al., 2015] were applied. An accuracy of 0.94 was provided by a two-view analysis, with specificity and sensitivity of 0.88 and 1 respectively. The author had admitted that the performance could be

further improved with CAD tools which have not been attempted.

L1-L2 SVM [Bing-Yu Sun et.al., 2011] was utilized as a valuable classification technique for regression analysis and had exposed automatic feature selection with fine classification performance. Seven prognostic prediction methods were used to compare with the proposed method. The efficiency and automation process need to be improved further, which had been accepted in the work.

The proposed algorithm was Vector-valued regularized kernel function approximation (VVRKFA) [Santanu Ghorai et.al., 2010]. Depending on the proximity to class centroids, a test pattern was classified. To compare for accuracy, a multiclass SVM was used. When compared to that of the multiclass SVM, though VVRKFA had been the better classifier, generalization capability was not considered.

### **Dataset of mammogram images**

Mammographic images were obtained from the digital database for screening mammography (DDSM)

[<http://marathon.csee.usf.edu/Mammography/Database.html>]. The DDSM is a database of digitized film-screen mammograms. This dataset provides a large set of mammograms in digital format. The website for DDSM [ <http://marathon.csee.usf.edu/Mammography/Database.html> ] is a resource with a large database. The texture and shape features are extracted from the mammogram images and these features are given to train the network. To extract the features, Local Binary Pattern (LBP) reconstructed image of each mammogram image is used. The texture and shape features are the best parameters used for the analysis of the mammogram images. Mammography is a technique which uses a less dosage of x-ray for the detection of breast tissue tumor. Even tumors of size 3mm can be detected using this technique. Based on research it is found that women who are in 50s and above are highly affected by breast cancer. An efficient method for the analysis of breast cancer is mammography since women fall in this group has breast tissues of low density which makes it as the most reasonable tool to detect early stage of breast cancer.

## **II. CMANTEC ALGORITHM**

CMantec is one of the recent neural network constructive algorithms with excellent prediction abilities that generate compact size neural architectures [Francisco Ortega-Zamorano, 2013]. The Cmantec Neural Network (CNN) similar to

other networks maps inputs to the output with the help of a hidden layer. The CNN applies thermal perceptron learning rule. This perceptron technique uses linear individual threshold units for training in order to find the optimized parameter. This technique uses separate gradient weight measurement for each unit with the corresponding neighbor unit to find the correlation between each unit. The difference between standard perceptron learning rule with thermal perceptron learning rule is that the later one uses a temperature factor which is denoted as  $T_{fac}$ .

### A. Thermal perceptron rule

Frean introduced thermal perceptron rule in 1992 [Marcus Frean, 1992], a modified perceptron rule. Consider a neuron which receives from  $N$  incoming signals and with two states of output: OFF/FALSE for 0 and ON/TRUE for 1. The activation state ( $S$ ) depends on  $N$  input signals, corresponding input  $\Psi_i$ , synaptic weights ( $w_i$ ) and bias ( $b$ ). The mathematical model implemented in this work is given below:

### Mathematical Modeling for C-Mantec using Thermal perceptron

$$f: R^N \rightarrow R$$

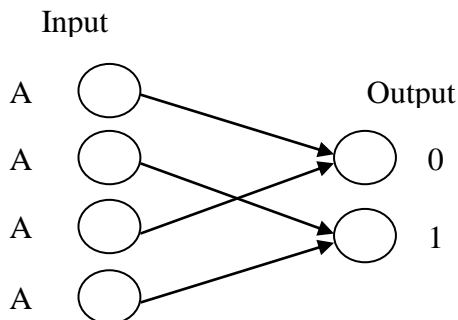
where,  $f$  - function to be learned,  $R^N$  - input vector of  $N$  dimensions &  $R$  - output vector of assumed one dimension. So, Output - Input pair is given by,

$$Y = \{(x^N, y) : x^N \in R^N, y \in R\}$$

where,  $x^N$  - specific  $N$ -dimensional input in  $R^N$  &  $y$  - output (one-dimensional).

Here, the function is one of the two discrete classes 0 / 1. i.e.,  $Y = \{0, 1\}$ . Therefore, thermal perceptron rule is used. Here,  $Y$  is the output mapping to the input.

$$Y = \{1 \text{ (ON), if } P \geq 0 \\ 0, \text{ otherwise}\}$$



Assuming that the inputs are stored in an array  $A[i]$ .

So,  $\{i \rightarrow 0 \text{ to } N - 1 \text{ for } A[i]\}$  with  $N$  - number of images (unique)  $P \Rightarrow w_i A_i - B$

where,  $P$  - synaptic potential of the neuron,  $w_i$  - weights of input  $A[i]$  &  $B$  - bias.

For normal perceptron the weight adjustment is as

$$\Delta w_i = l(X_i - Y_i) * A_i$$

where  $l$  - learning rate ( how fast it learns),  $X_i$  - target ( from training data) &  $Y_i$  - output prediction.

### For Thermal Perceptron,

$T = T_0 - M_I$ , with initial Temperature as  $T_0$  and (Number of input variables).

$M \rightarrow$  Variable to set  $T \Rightarrow 0 \forall I = I_{max}$

Now, let's compute  $T_{fac}$  (health factor) as  $T_{fac} = \frac{T}{T_0} \exp\{-\frac{|P|}{T}\}$  which is the change in factor for the thermal perception learning rule.

$$\Delta W_i = (X_i - Y_i) * P * T_{fac}$$

i.e., weight change,  $\Delta W_i \Rightarrow$  (target-output) \* synaptic potential\* health factor.

### C-mantec using thermal perceptron

Let's consider  $S_t$  as entire patterns in the training dataset. Process completion would be marked by

$$X_i - Y_i \text{ for all } \forall S_t, 0 \leq t \leq C_n.$$

Here,  $C_n \rightarrow$  total number of patterns.

Now, the selection of  $rand(S_t)$  takes place.  $X_i \neq Y_i$  for  $S_t$  where  $t = rand(S_t)$ .

Then the sorting of neurons  $n_t$  with respect to  $T_{fac}$  takes place &  $\max(T_{fac})$  is selected.

A new factor  $G_{fac}$  is included, which will be the threshold for usefulness.

$$\text{Add} \Rightarrow \begin{cases} n_{t+1} \leftarrow n_t, & T_{fac} > G_{fac} \\ n_t, & \text{otherwise} \end{cases}$$

Now, process completion is checked again.

### SLBP Procedure

Texture features are extracted from the mammogram images using SLBP [Jeonghyun Baek et.al., 2014] instead of LBP (Linear Binary Pattern). These features are extracted because the mammogram images are properly analyzed using these features. The various texture features extracted are: Energy,

Contrast, Correlation, Homogeneity, Mean, RMS, SD, Entropy, etc.

The following steps are used to extract the texture features:

- 1) Every pixel is considered as the center pixel in the local region by swapping the position of the center pixel and the adjacent pixel.
- 2) LBP is applied with respect to the center pixel.
- 3) Binary string of LBP is obtained from previous step.
- 4) The obtained binary string is then given to the network for training.

Texture analysis plays an important role in detecting the disease pattern in mammogram. Linear Binary Pattern (LBP) is considered as an excellent method for processing because no textural information is lost. However, in the local region these LBPs miss the association amongst all of the pixels. So, Support LBP (SLBP) is introduced to establish this relationship.

This enhances the existing LBP's performance and also improves the classification generalization [Jeonghyun Baek et. al., 2014]. Thus, it is evident that the performance of current local pattern can be improved by establishing a full relationship between local region pixels. Binary string is developed by comparing the adjacent pixel with the current center pixel. If the adjacent pixel value is less than or equal to the center pixel then, the adjacent pixel value is replaced as 'zero'. Otherwise, the adjacent pixel value remains as 'one'. Here every pixel acts as a center pixel in the local region.

The schematic diagram of binary string generation and pixel swapping from 00 to 1350 as a sample work is shown below:

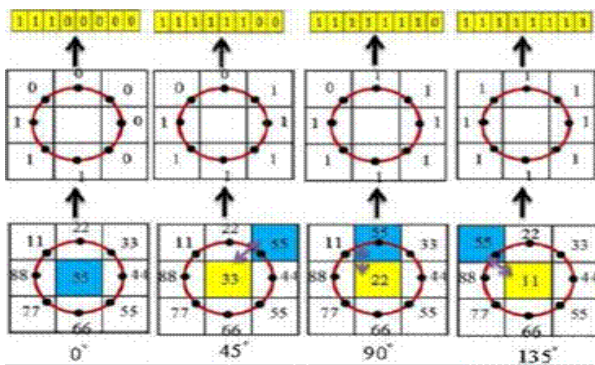


Fig. 1. Pixel swapping and generation of a binary string

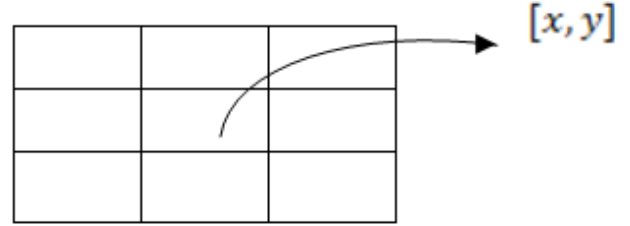
## Local binary pattern

This is to analyze the real input from image, a DICOM file or PNG file.

Consider an array of 2D size  $A[28][28]$ .

To apply SBLP, where all the transformation are taking place, all transforms have to be combined.

## LBP (Linear Binary Pattern)



Consider centre pixel as  $A[x, y]$ .

So,

$$A_1 \leftarrow A[x - 1, y - 1]$$

$$A_2 \leftarrow A[x, y - 1]$$

$$A_3 \leftarrow A[x + 1, y - 1]$$

$$A_4 \leftarrow A[x - 1, y]$$

$$A_5 \leftarrow A[x, y]$$

$$A_6 \leftarrow A[x + 1, y]$$

$$A_7 \leftarrow A[x - 1, y + 1]$$

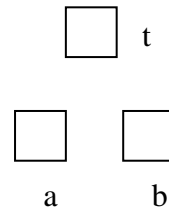
$$A_8 \leftarrow A[x, y + 1]$$

$$A_9 \leftarrow A[x + 1, y + 1]$$

Let's define eight states

$$C_\theta = 0^\circ, C_\theta = 45^\circ, C_\theta = 90^\circ, C_\theta = 135^\circ, C_\theta = 180^\circ, C_\theta = 225^\circ, C_\theta = 270^\circ, C_\theta = 315^\circ$$

Consider:



Define 2 functions:

$$swap(a, b) = \begin{cases} t = a \\ b = a \\ a = t \end{cases}$$

### Check LBP

$$\begin{pmatrix} x, y \\ x1, y1 \end{pmatrix} = \begin{cases} A[x1, y1] > A[x, y], A[x, y1] = 1 \\ A[x, y1] < A[x, y], A[x, y] = 0 \end{cases}$$

For  $\theta = 0^\circ$ :

$$C_\theta = 0^\circ \Rightarrow \begin{cases} \text{swap}(A_5, A_5) \\ \text{check LBP}(A_5, A_{1-9}) \end{cases}$$

$$C_\theta = 45^\circ \Rightarrow \begin{cases} \text{swap}(A_5, A_3) \\ \text{check LBP}(A_5, A_{1-9}) \end{cases}$$

$$C_\theta = 90^\circ \Rightarrow \begin{cases} \text{swap}(A_5, A_2) \\ \text{check LBP}(A_5, A_{1-9}) \end{cases}$$

$$C_\theta = 135^\circ \Rightarrow \begin{cases} \text{swap}(A_5, A_1) \\ \text{check LBP}(A_5, A_{1-9}) \end{cases}$$

$$C_\theta = 180^\circ \Rightarrow \begin{cases} \text{swap}(A_4, A_5) \\ \text{check LBP}(A_5, A_{1-9}) \end{cases}$$

$$C_\theta = 225^\circ \Rightarrow \begin{cases} \text{swap}(A_5, A_7) \\ \text{check LBP}(A_5, A_{1-9}) \end{cases}$$

$$C_\theta = 270^\circ \Rightarrow \begin{cases} \text{swap}(A_5, A_8) \\ \text{check LBP}(A_5, A_{1-9}) \end{cases}$$

$$C_\theta = 300^\circ \Rightarrow \begin{cases} \text{swap}(A_5, A_6) \\ \text{check LBP}(A_5, A_{1-9}) \end{cases}$$

$$C_\theta = 315^\circ \Rightarrow \begin{cases} \text{swap}(A_5, A_9) \\ \text{check LBP}(A_5, A_{1-9}) \end{cases}$$

C  $\Rightarrow$  is a histogram.

### Support Local binary pattern

Now,  $\text{Join hist}(C_1, C_2) = \{c_1[x, y] + C_2[x, y]$

$$\begin{aligned} &\text{Join hist}(\text{Join hist}(C_{\theta=45^\circ}, C_{\theta=90^\circ}) \\ &+ \text{Join hist}(C_{\theta=135^\circ}, C_{\theta=180^\circ})) \\ &+ \text{Join hist}(\text{Join hist}(C_{\theta=225^\circ}, C_{\theta=275^\circ}) \\ &+ \text{Joint hist}(C_{\theta=315^\circ}, C_{\theta=360^\circ})) \end{aligned}$$

$$\text{SLBP} \Rightarrow \text{Joint hist}(C_0, C_{0-360^\circ})$$

This along with Image processing like Binarization, Background, Noise reduction of segmentation will give us the unique input  $A_i$ .

Finally SLBP into C-Mantec :

$A_i$  is obtained from SLBP and therefore assume an example set of  $A_i$

	ID1	ID2	ID3	ID4
$A_i =$	1.2	1.4	1.9	2.3]
$X_i =$	[0	0	1	1]
	A	B	C	D

$X_i$  - cancer output.

w.k.t,

$$P \Rightarrow w_i A_i - B$$

Let  $B = 1.5$ ,

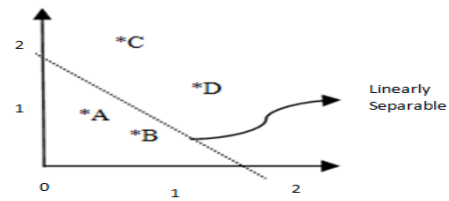
$$0 = w_i * 1.2 - 1.5$$

$$0 = w_i * 1.4 - 1.5$$

$$1 = w_i * 1.9 - 1.5$$

$$1 = w_i * 2.3 - 1.5$$

After training phase,



Now an image is taken which has no output for (test set).

Two cases:

$$A_i = 0.9, A_i = 2$$

$$Y_i = \begin{cases} 1, & P \geq 0 \\ 0, & \text{otherwise} \end{cases}$$

$$w_i = +1$$

For Case 1:  $P = (+1)(0.9) - 1.5 = -0.6$ , and  $P \leq 0$

For Case 2:  $P = (+1)(0.9) - 1.5 = 0.5$ , and  $P \geq 0$

Therefore,

In Case 1 ( $A_i = 0.9$ ):  $Y_i = 0 \Rightarrow$  NO CANCER

In Case 1 ( $A_i = 2$ ):  $Y_i = 1 \Rightarrow$  CANCER IS PRESENT

To calculate the values of various parameters chosen, Binarization formulae is used.

### Binarization Formulae

Energy of an image

$$E_{\text{img}} = \int_{-\infty}^{\infty} |x(t)|^2 dt \quad (6)$$

where  $x$  is the pixels in the image.

Entropy of an image

$$H = - \sum_k P_k \log_2(P_k) \quad (7)$$

where  $H$  is the entropy of the image,  $P_k$  is the probability of the gray level  $k$  of the image.

Standard deviation

$$\sigma = \sqrt{\frac{1}{N} \sum_{i=1}^N (x_i - \mu)^2} \quad (8)$$

where  $\sigma$  is standard deviation of the image,  $N$  is the pixel count in the image and  $\mu$ , mean of an image.

Mean

$$\mu = \frac{\sum_{i=1}^N x_i}{N} \quad (9)$$

where  $x_i$  is the value of a pixel,  $N$  is the total count of pixels and  $\mu$ , mean of an image.

Correlation

$$r = \frac{N \sum xy - (\sum x)(\sum y)}{\sqrt{[N \sum x^2 - (\sum x)^2][N \sum y^2 - (\sum y)^2]}} \quad (10)$$

$r$  is correlation value,  $x$  is the input image and  $y$  is the output image,  $N$  is the number of pixels.

Homogeneity

$$\text{Homogeneity} = \sum_i \sum_j \frac{P[i,j]}{1+|i-j|} \quad (11)$$

where  $P$  is the image,  $i$  and  $j$  are row and column values of the image.

For  $i=1: N$   
if  $r(i) > r(k-2)$   
 $r(i) == 1;$   
else  
 $r(i) == 0;$   
end

The first pixel to be considered for iteration is planned by Table1.

Table 1. Pixel block in binarization

Deg	0	45	90	135	180	225	270
Pixel order in each binarization	r(k-3)	r(k-2)	r(k+1)	r(k+4)	r(k+3)	r(k+2)	r(k-1)
	r(k-2)	r(k+1)	r(k+4)	r(k+3)	r(k+2)	r(k-1)	r(k-4)
	r(k+1)	r(k+4)	r(k+3)	r(k+2)	r(k-1)	r(k-4)	r(k-3)
	r(k+4)	r(k+3)	r(k+2)	r(k-1)	r(k-4)	r(k-3)	r(k-2)
	r(k+3)	r(k+2)	r(k-1)	r(k-4)	r(k-3)	r(k-2)	r(k+1)
	r(k+2)	r(k-1)	r(k-4)	r(k-3)	r(k-2)	r(k+1)	r(k+4)
	r(k-1)	r(k-4)	r(k-3)	r(k-2)	r(k+1)	r(k+4)	r(k+3)
	r(k-4)	r(k-3)	r(k-2)	r(k+1)	r(k+4)	r(k+3)	r(k+2)

### Cmantec Algorithm formula

To find the LBP output image, pixels in the image are separated into many pixel blocks. The number of pixels in the block is separated by order of two ( $x^2$ ). Therefore, the center pixel is taken as the reference pixel and weight and synoptic potential are calculated with the surrounding pixels.

$$k = \left\lceil \frac{N+1}{2} \right\rceil r \quad (12)$$

where  $r$  is the image block,  $r(k)$  is the center pixel of the image.

$N$  is the entire pixel count in a block.

$k$  – Iterations

After calculation of weight and potential of that image pixel, the value of pixels that are above the weight of center pixels is considered as 1. This technique is called as binarization; it can be used as group image pixel so that computation can be done effectively. The general formula of binarization is given as follows.

### Binarization:

For  $i=1: N$   
if  $r(i) > r(k-3)$   
 $r(i) == 1;$   
else  
 $r(i) == 0;$   
end

The iteration will be decided on the basis of Table 2.

Table 2. Iteration decision table

0	45	90	135	180	225	270	315
k-3	k-2	k+1	k+4	k+3	k+2	k-1	k-4

Therefore the iteration will be taken for each value in the table to find the result.

$0^0$  rule

For  $i = k-3 : N-1$   
For  $j = 1 : k-3$   
 $X(i)=r(i);$   
 $a = a + 1;$   
 $X(a+j) = r(j);$   
end  
end

$45^0$  rule

For  $i = k-2 : N-1$   
For  $j = 1 : k-2$   
 $X(i)=r(i);$   
 $a = a + 1;$   
 $X(a+j) = r(j);$   
end  
end

90° rule

```

For i = k+1 : N-1
For j = 1 : k+1
    X(i)=r(i);
    a = a + 1;
    X(a+j) = r(j);
end
end

```

135° rule

```

For i = k+4 : N-1
For j = 1 : k+4
    X(i)=r(i);
    a = a + 1;
    X(a+j) = r(j);
end
end

```

180° rule

```

For i = k+3 : N-1
For j = 1 : k+3
    X(i)=r(i);
    a = a + 1;
    X(a+j) = r(j);
end
end

```

225° rule

```

For i = k+2 : N-1
For j = 1 : k+2
    X(i)=r(i);
    a = a + 1;
    X(a+j) = r(j);
end
end

```

270° rule

```

For i = k-1 : N-1
For j = 1 : k-1
    X(i)=r(i);
    a = a + 1;
    X(a+j) = r(j);
end
end

```

315° rule

```

For i = k-4 : N-1
For j = 1 : k-4
    X(i)=r(i);
    a = a + 1;
    X(a+j) = r(j);
end
end

```

Result

$$X(\text{req result}) = X(0) + X(45) + X(90) + X(135) + X(180) + X(225) + X(270) + X(315) + X(360).$$

The flow chart of Cmantec is given below:

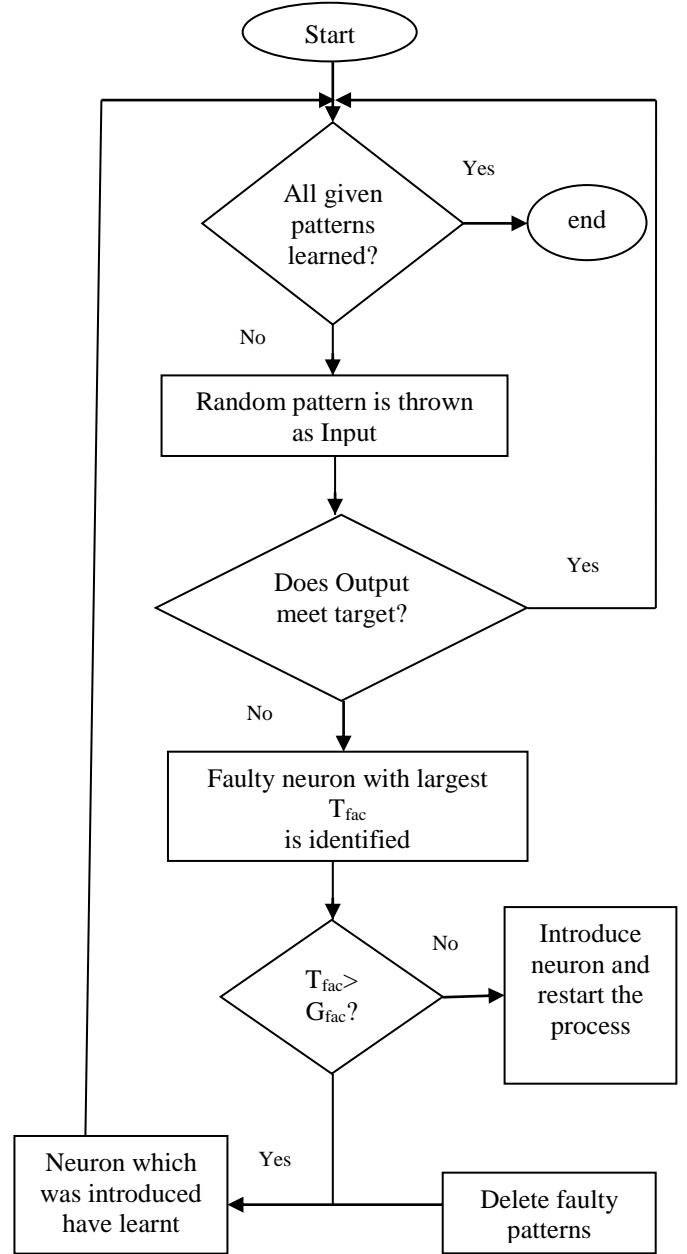


Fig. 2. CMantec algorithm's flow chart

Finally, thermal perceptron learning rule helps out to learn patterns and are able to classify the normal and abnormal mammogram images. Therefore, by using the constructive neural networks a novel neural architecture can be constructed without overfitting or underfitting. The input parameters are given to the network for training.



After training, a new input is given to the network and check whether the output is equal to target. If it is not equal, the faulty neuron with largest Tfacs is selected. If Tfacs is greater than Gfacs, then the selected neuron learns the pattern otherwise additional neuron is introduced to the network. This procedure is continued until all the patterns are learned by the network.

## RESULTS AND CONCLUSION

The mammogram images are used as the input from which the texture and shape features are extracted and these parameters are used for training the network. The network is now trained with normal mammogram images. Finally after getting trained, when a new image is given to the network, it should be classified. If the input given is a normal mammogram image, then the output will be “detected with subjective classification” whereas, if the input image given is an abnormal mammogram, then the output will be “detection failed”. The improvement of generalization capability along with speed [J.Jeya Caleb and M.Kannan , 2017] is also obtained in the diagnosis of a skin cancer.

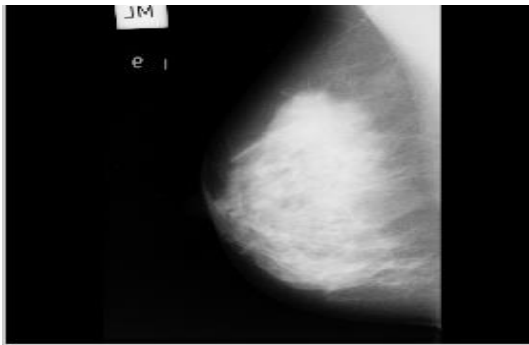


Fig. 3. Normal mammogram image

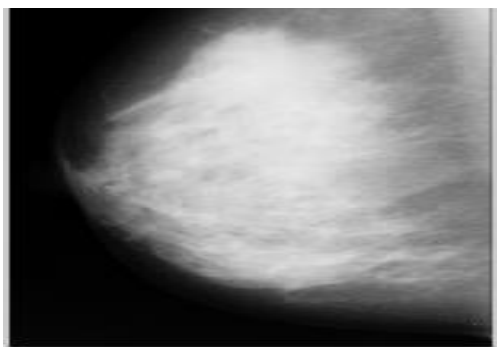


Fig. 4. Cropped image

The input image taken from the mammogram database consists of dark regions that are not necessary for cancer recognition. They are removed from the image to increase the computational efficiency. The cropped image and input image are shown in figure 3 and 4 respectively.

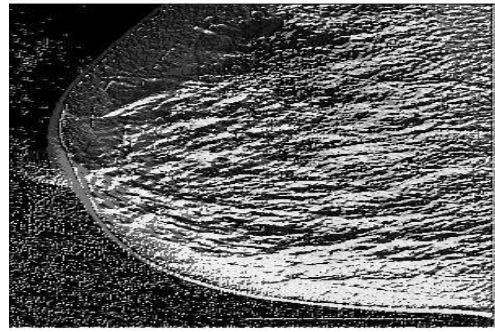


Fig. 5. LBP reconstructed output image

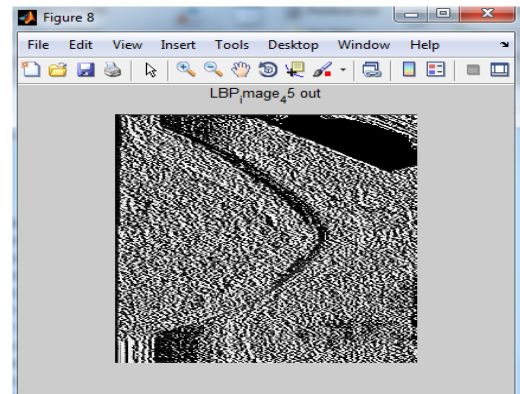


Fig. 6. LBP image at 450

To find the cancer feature from the image, the order of binarization is initialized and each pixel in the image is converted into a binary cell using binarization principle as shown in figure 5.

All the  $(x^2 - 1)$  combination of binarization are calculated and they are summed to form the final output as in figure 6. This can be used to collect texture from the image.

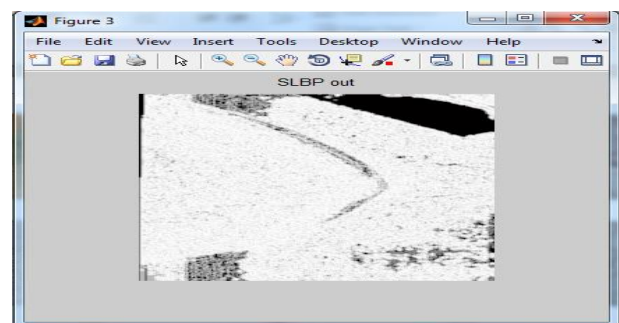


Fig. 7. SLBP output

The results are then compared with existing LBP algorithm to find the efficiency of the cancer recognition. The output in figure 7 shows the features, that are extracted from the input image. This extracted features are then classified using neural networks. For further testing, a set of images were taken into consideration and they were given as an input to the algorithm and the corresponding outputs were obtained, which were shown as:



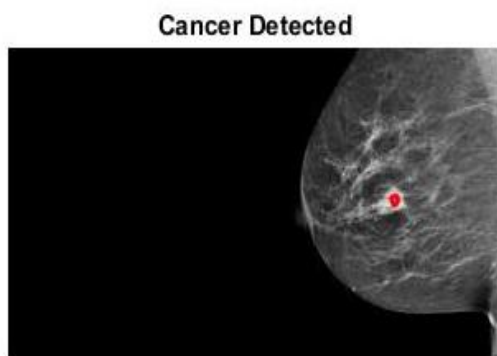


Fig. 8. (Cancer1) – Cancer Detected Image

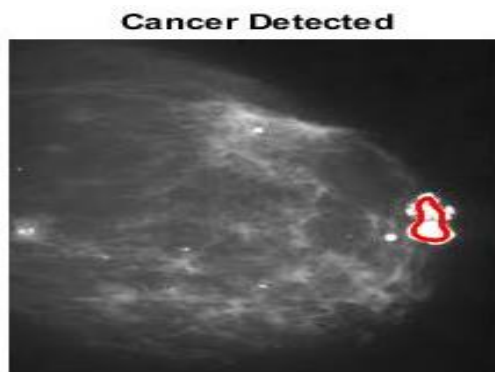


Fig. 12. (Cancer5) – Cancer Detected Image

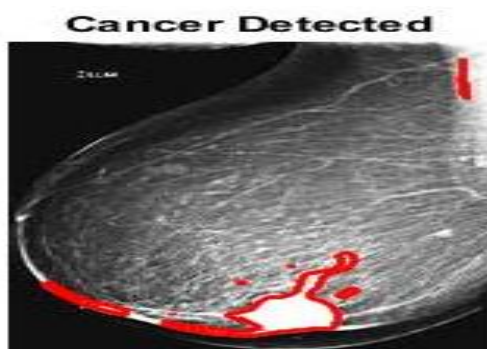


Fig. 9. (Cancer2) – Cancer Detected Image

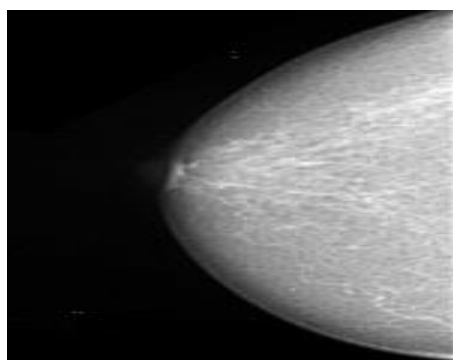


Fig. 13 (Norm1) – Non-Cancer Image

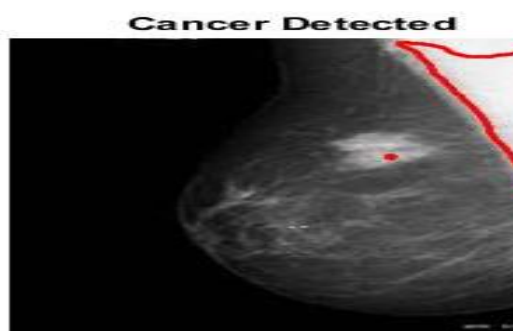


Figure 10. (Cancer3) – Cancer Detected Image

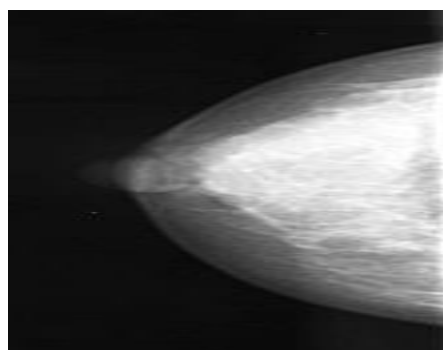


Fig. 14. (Norm2) – Non Cancer Image

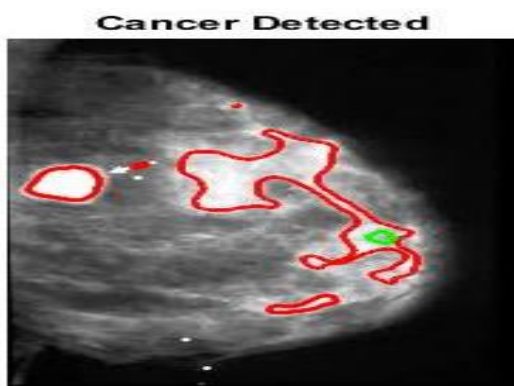


Fig. 11. (Cancer4) – Cancer Detected Image

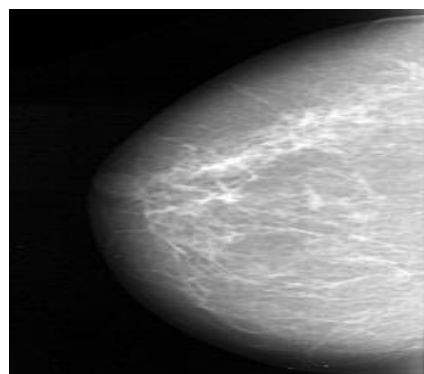


Fig. 15. (Norm3) – Non Cancer Image

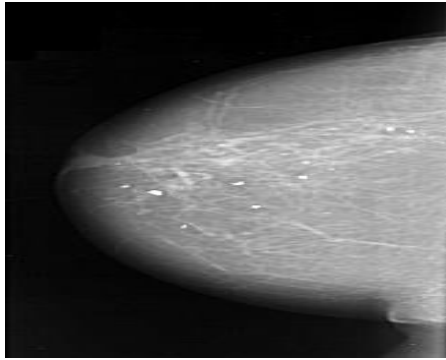


Fig. 16. (Norm4) – Cancerless Image

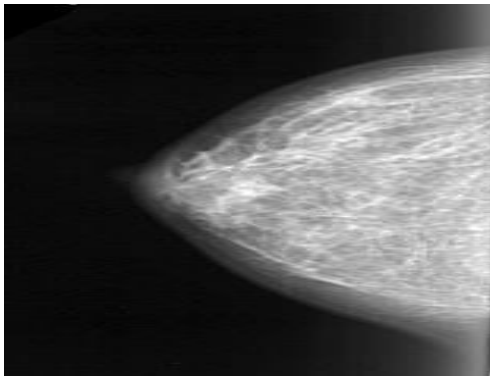


Fig. 17. (Norm5) – Non Cancer Image

Output graphs obtained by comparing the above set of images for various texture features were displayed as:

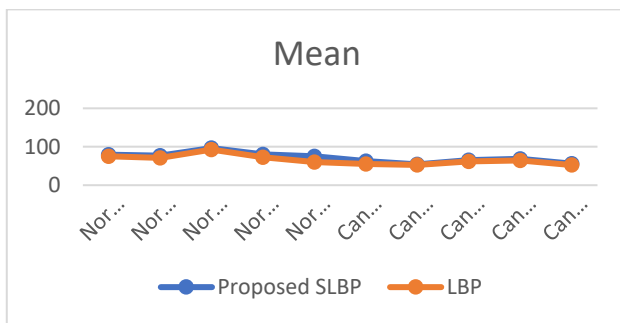


Fig. 18. Mean Value of the images

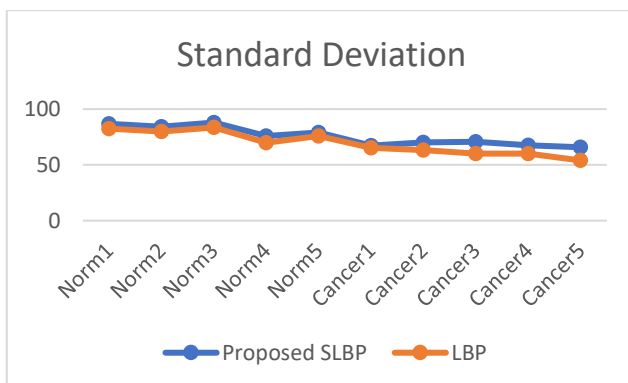


Fig.19. Standard Deviation of the images

Mean and standard deviation of the image is given in figure 18 & 19 respectively. It is used to find the contribution of each pixel to the neighboring pixels and thereby it also assists in evaluating the different class orientation of the image. From the above figures 18 & 19, it is shown that normal image has more deviation when compared to abnormal images.

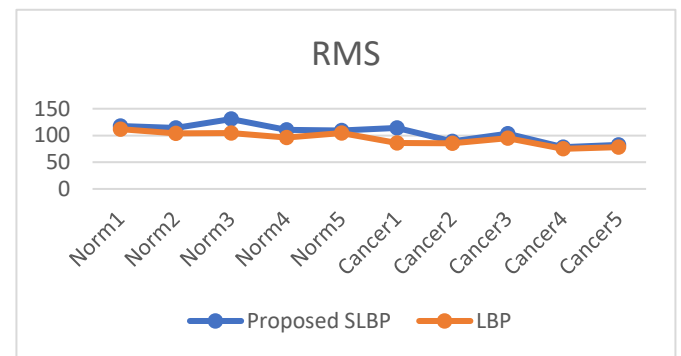


Fig. 20. RMS value of the images

The above figure 20 is used to find the mean of a set of numbers. It is shown that normal image with high mean has higher RMS values.

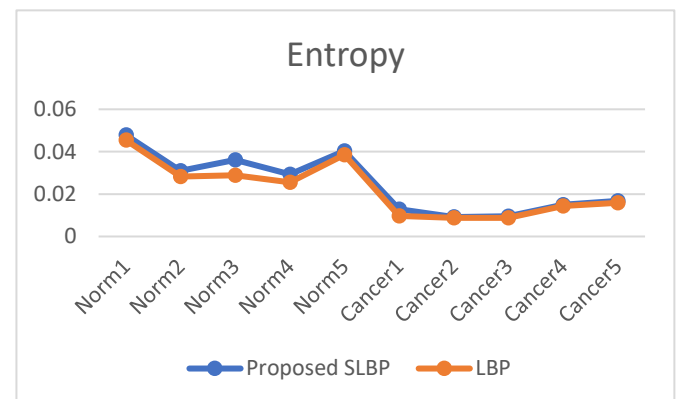


Fig. 21. Entropy of the images

Entropy is the measure of the energy of the image. It is clear from figure 21 that normal image has higher entropy when compared with abnormal images. Figure 22 show that normal images have more association when compared with abnormal images.

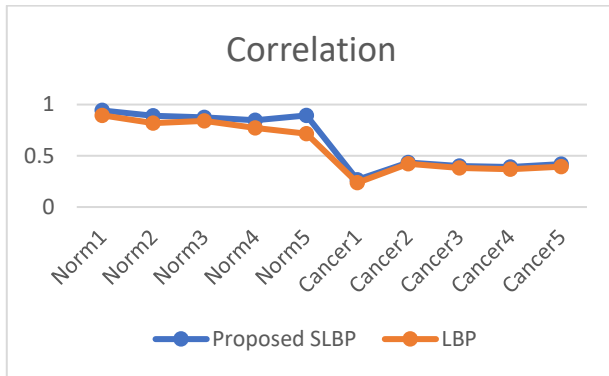


Fig. 22. Correlation of the images

Homogeneity is the measure of uniqueness of image. Figure 23 shows that normal images are more unique when compared with cancerous images especially in SLBP technique.

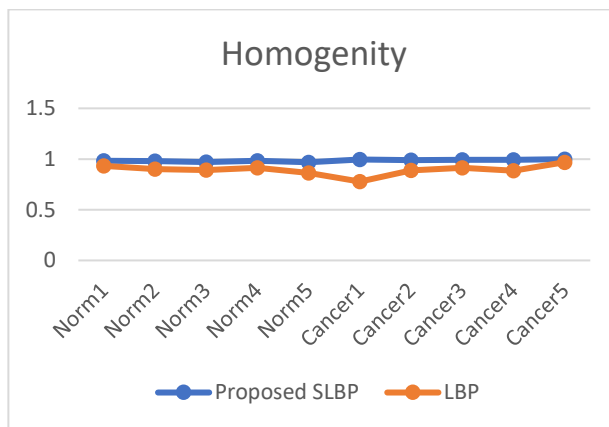


Fig. 23. Homogeneity of the images

The table with various texture feature values obtained for a variety of images is listed as following in Table 3 and 4.

Table 3. Figures of merit

DATA	Proposed	LBP	Proposed	LBP	Proposed	LBP
	Mean		SD		RMS	
Norm 1	79.53	75.55	86.82	82.48	117.74	11.85
Norm 2	76.99	70.83	84.08	79.88	114.00	10.374
Norm 3	96.55	92.68	87.96	83.56	130.61	10.449
Norm 4	80.07	72.86	76.02	69.94	110.41	96.06
Norm 5	75.62	60.50	78.94	75.78	109.32	10.440

Cancer 1	62.37	55.51	67.24	65.22	114.25	85.69
Cancer 2	54.24	52.61	70.14	63.12	88.66	85.12
Cancer 3	65.31	62.04	70.83	60.21	103.38	95.11
Cancer 4	68.42	64.70	67.65	60.21	78.10	74.97
Cancer 5	55.78	52.44	65.78	53.94	82.58	78.04

Table 4. Figures of merit

DATA	Proposed	LBP	Proposed	LBP	Proposed	LBP
	Entropy		Correlation		Homogeneity	
Norm 1	0.05	0.05	0.94	0.90	0.98	0.93
Norm 2	0.03	0.03	0.89	0.82	0.98	0.90
Norm 3	0.04	0.03	0.88	0.84	0.97	0.89
Norm 4	0.03	0.03	0.85	0.77	0.98	0.91
Norm 5	0.04	0.04	0.90	0.72	0.97	0.86
Cancer 1	0.01	0.01	0.27	0.24	1.00	0.78
Cancer 2	0.01	0.01	0.44	0.42	0.99	0.89
Cancer 3	0.01	0.01	0.40	0.38	0.99	0.91
Cancer 4	0.02	0.01	0.39	0.37	0.99	0.88
Cancer 5	0.02	0.02	0.42	0.39	1.00	0.97

After training and testing the network, when a new input is given, the output is displayed as shown in Fig. 28 and Fig.29:

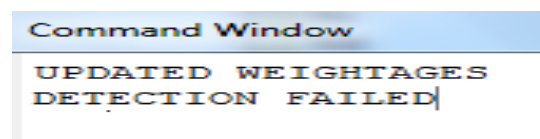


Fig. 28. Output displayed when normal mammogram image is given

```

Command Window
>> TRAINCLASSIFY
UPDATED WEIGHTAGES
DETECTED with subjective clasiffication

```

Fig. 29. Output displayed when abnormal mammogram image is given

## CONCLUSION

As described herein, using the novel CMANTEC algorithm, the error in detecting breast cancer for patients is reduced. The accuracy of cancer detection with proposed algorithm is about 98.5% which is high when compared to other existing algorithms. The database for cancer detection is taken from the University of South Florida mammogram database. The data was divided into two sets as test set and training set. The data in training set are trained with the help of CMANTEC algorithm and compared with a test set. This technique can also be used in real time applications such as IoT and wearable technologies.

## REFERENCES

- [1] Bing-Yu Sun, Zhi-Hua Zhu, Jiuyong Li, et.al. "Combined Feature Selection and Cancer Prognosis Using Support Vector Machine Regression," *Journal IEEE/ACM Transactions on Computational Biology and Bioinformatics*, vol.8 no.6, pp.1671-1677, 2011.
- [2] Chih-Min Lin, Yu-Ling Hou, Te-Yu Chen, et.al. "Breast Nodules Computer-Aided Diagnostic System Design Using Fuzzy Cerebellar Model Neural Networks," *IEEE transactions on fuzzy systems*, vol. 22, no. 3, pp. 693-698, 2014.
- [3] Chih-Min Lin and Hsin-Yi Li, "Intelligent hybrid control system design for antilock braking systems using self-organizing function-link fuzzy cerebellar model articulation controller," *IEEE transactions on fuzzy systems*, vol. 21, no.6, pp. 1044-1055, 2013.
- [4] Daniel Urda, Jose Luis Subirats, Leo Franco, et al., "Constructive Neural Networks to predict breast cancer outcome by gene expression profiles," Springer, 2010.
- [5] Francisco Ortega-Zamorano, José Luis Subirats, José Manuel Jerez, Ignacio Molina, et.al., "Implementation of the C-Mantec Neural Network Constructive Algorithm in an Arduino Uno Microcontroller," *International Conference on Artificial Neural Networks*, IWANN Springer, pp.80-87, 2013.
- [6] <http://marathon.csee.usf.edu/Mammography/Databas e.html>.
- [7] Hung-Yi Hsieh and Kea-Tiong Tang, "Hardware Friendly Probabilistic Spiking Neural Network with Long-Term and Short-Term Plasticity," *IEEE transactions on neural networks and learning systems*, vol. 24, no.12, pp. 2063- 2073, 2013.
- [8] Jeonghyun Baek, Jisu Kim and Euntai Kim, "Part-based face detection using SLBP International Conference on Control," *Automation and Systems (ICCAS)*, pp.1501 – 1503, 2014.
- [9] J.Jeya Caleb and M.Kannan, "Efficient VLSI Implementation of the C-MANTEC Conn Algorithm by Using PID Controllers," *Circuits and Systems (Scientific Research Publishing)*, vol. 8, no. 11, pp. 253-260, 2017.
- [10] Marcus Frean, "A Thermal Perceptron Learning Rule," *Neural Computation, The MIT Press Journals*, November vol. 4, no.6, pp.946-957, 1992.
- [11] Mohammad Sameti, Rabab Kreidieh Ward, Jacqueline Morgan-Parkes, et.al. "Image Feature Extraction in the Last Screening Mammograms Prior to Detection of Breast Cancer," *IEEE Journal of selected topics in Signal Processing*, vol. 3, no. 1, pp. 46 – 52, 2009.
- [12] Paola Casti, Arianna Mencattini, Marcello Salmeri, et.al, "Analysis of Structural Similarity in Mammograms for Detection of Bilateral Asymmetry," *IEEE Transactions on Medical Imaging*, vol. 33, no.9, pp.1- 3, 2015.
- [13] Santanu Ghorai, Anirban Mukherjee, and Pranab K. Dutta, "Discriminant Analysis for Fast Multiclass Data Classification through Regularized Kernel Function Approximation," *IEEE transactions on Neural Networks*, vol. 21, no.6, pp.1020- 1029, 2010.
- [14] Tzyy-Chyang Lu, Gwo-Ruey Yu and Jyh-Ching Juang, "Quantum-Based Algorithm for Optimizing Artificial Neural Networks," *IEEE transactions on Neural Networks and Learning Systems*, vol. 24, no.8, pp.1266-1278, 2013.
- [15] Vikraman Baskaran, Aziz Guergachi, Rajeev K. Bali, et.al. "Predicting Breast Screening Attendance Using Machine Learning Techniques," *IEEE transactions on Information Technology in Biomedicine*, vol. 15, no. 2, pp. 251- 259, 2011.